S.M. López Silva, J.P. Silveira and M.L. Dotor
Test of a processing algorithm for NIR laser diodes based pulse oximetry

This paper was published in
Proceedings of SPIE Vol. 5119, *Bioengineered and Bioinspired Systems*, edited by Angel Rodríguez-Vázquez, Derek Abbott, Ricardo Carmona (SPIE, Bellingham, WA, 2003) pp. 178-188, and is made available as an electronic reprint with permission of SPIE.

Test of a processing algorithm for NIR laser diodes based pulse oximetry

Sonnia María López Silva[a], Juan Pedro Silveira[b], María Luisa Dotor[b]

[a]Instituto Universitario de Microelectrónica Aplicada, Universidad de Las Palmas de Gran Canaria, Las Palmas de Gran Canaria 35017, Spain;
[b]Instituto de Microelectrónica de Madrid, CNM, CSIC, Madrid 28760, Spain.

ABSTRACT

Pulse oximeters are used for the non-invasive monitoring of arterial blood haemoglobin oxygen saturation. The photoplethysmographic (PPG) signals measured at two specific wavelengths are decomposed into its variable (E_{AC}) and the constant component (E_{DC}) for deriving a parameter related to the arterial blood oxygen saturation (So_2). Previously it has been reported a signal processing algorithm for a near infrared (NIR) laser diodes based transmittance pulse oximetry system. The proposed algorithm permits the numeric separation of the variable and constant parts of the signals for two wavelengths, to derive a quotient (q) proportional to the So_2 levels. The E_{DC} is obtained by a low pass filtering and E_{AC} by a pass-band one, followed by a non-linear filtering. The non-linear filter is based on the reduction of the E_{AC} peak-to-peak frequency distribution for the analyzed time interval (histogram reduction). In the present study is exposed the influence of Bessel filters cut-off frequencies and histogram reduction percentage on q values. The test has been conducted on PPG signals recorded through experimental studies on human healthy volunteers using the NIR laser diodes based transmittance pulse oximetry system. The sources of artefacts and noise in the laser diodes PPG signals are discussed.

Keywords: biomedical signal processing, pulse oximetry, photoplethysmography, laser diodes, near infrared

1. INTRODUCTION

Pulse oximeters are widely used for the non-invasive monitoring of arterial blood haemoglobin oxygen saturation (So_2)[1-6]. This technique is based on the time variable optical attenuation by a vascular bed due to the cardiac pumping action (photoplethysmography)[7-9] and the differential optical absorption of the oxy- and deoxy-hemoglobin[10-12]. The photoplethysmographic (PPG) signals measured at two specific wavelengths are decomposed into its variable or pulsating component (E_{AC}) and the constant or non-pulsating component (E_{DC}) for deriving a parameter related to the arterial blood oxygen saturation (So_2). The classical pulse oximeters[4-6] use light emitting diodes (LEDs) as sources, with emissions in two regions of the optical spectrum, in the red (e.g. 660 nm) and in the infrared (880-940 nm).

Previously we reported the application to pulse oximetry of a measure system and a transmittance optical sensor based on two near infrared (NIR) laser diodes[13-19]. We also developed a real time processing algorithm[15, 16] that allowed us to analyze our sensor output and to derive a correct value of a parameter related to So_2 with good dynamic characteristics from the time variant detected signals. The main difficulties in the extraction of the information from the PPG signals are the small value of the signals variation related to their constant values, and the presence of artefacts caused by macro- and micro- movements of the part under analysis. The proposed algorithm permits the numeric separation of the variable and constant parts of the signals for both wavelengths to derive a quotient (q) proportional to the So_2 levels. The E_{DC} is obtained by a low pass filtering, and E_{AC} by a pass-band one, followed by a non-linear filtering based on histogram reduction. In the present study is exposed the influence of Bessel filters cut-off frequencies and histogram reduction percentage on q values. The test has been conducted on PPG signals recorded through experimental studies on human healthy volunteers using the NIR laser diodes based transmittance pulse oximetry system. Further to it, the sources of artefacts and noise in the laser diodes PPG signals are discussed.

2. MEASUREMENT PRINCIPLES, SYSTEM AND PROCESSING

2.1 Pulse oximetry principles

Oxygen saturation refers by definition to the part of haemoglobin concentration in the blood that can combine reversibly with oxygen[20] and is usually expressed as a percentage. Consequently

$$So_2 = \frac{c_{HbO_2}}{c_{tHb} - c_{dHb}} \times 100 = \frac{c_{HbO_2}}{c_{RHb} + c_{HbO_2}} \times 100, \quad (1)$$

being c_{tHb}, c_{dHb}, c_{HbO2} and c_{RHb} the concentrations of total haemoglobin, dyshaemoglobins, oxyhaemoglobin and deoxyhaemoglobin, respectively.

Pulse oximetry is based on the time variable optical attenuation by a vascular bed due to the cardiac pumping action (photoplethysmography) [7-9] and the differential optical absorption of the oxy- (HbO_2) and deoxyhaemoglobin (RHb) [10- 12]. This approach assumes that the time dependent photoplethysmographic signal is caused solely by changes in the arterial blood volume associated with the cardiac cycle and that no other hemoglobin derivatives different from HbO_2 or RHb are present. This signal is decomposed into its variable or pulsating component (E_{AC}) and the constant or non-pulsating component (E_{DC}). The variable component of the photoplethysmograms (PPG) results from the expansion and relaxation of the arterial bed, while the constant component is related to the attenuation by non-pulsating arterial blood, venous blood and tissues. Oxygen saturation is derived by analyzing the pulsating component peak-to-peak value (E_{AC}) of the PPG related to the corresponding constant component (E_{DC}) of the PPG, at two specific wavelengths. Some theoretical equations assume the validity of Beer-Lambert-Bouguer's law for deriving the relationship between oxygen saturation (So_2) and optical properties of a pulsating vascular bed as [2-4]:

$$So_2 = \frac{\varepsilon_{RHb}^{\lambda_1} - \varepsilon_{RHb}^{\lambda_2} \bullet q}{\varepsilon_{RHb}^{\lambda_1} - \varepsilon_{HbO_2}^{\lambda_1} - \left(\varepsilon_{RHb}^{\lambda_2} - \varepsilon_{HbO_2}^{\lambda_2}\right) \bullet q}, \quad (2)$$

where $\varepsilon_{RHb}^{\lambda_1}, \varepsilon_{HbO_2}^{\lambda_1}, \varepsilon_{RHb}^{\lambda_2}, \varepsilon_{HbO_2}^{\lambda_2}$ are the absorptivities or specific absorption coefficients of RHb and HbO_2 at wavelengths λ_1 and λ_2 respectively, and q is the ratio of the signals E_{AC} and E_{DC} for these wavelengths[2,3], which could be expressed as:

$$q = \frac{\log(1 - \frac{E_{AC}^{\lambda 1}}{E_{DC}^{\lambda 1}})}{\log(1 - \frac{E_{AC}^{\lambda 2}}{E_{DC}^{\lambda 2}})} \approx \frac{\frac{E_{AC}^{\lambda 1}}{E_{DC}^{\lambda 1}}}{\frac{E_{AC}^{\lambda 2}}{E_{DC}^{\lambda 2}}}. \quad (3)$$

The attenuation of the radiation by a pulsating bed is due to the blood RHb and HbO_2 absorption, but multiple scattering in the tissue structures and red blood cells also contributes to it. Thus, in a real situation, the Eq. (2) is an approximation and many studies have attempted to obtain more realistic models both for transmittance and reflectance modes. From a practical point of view, a typical relationship used for calibrating pulse oximeters has the form[21]

$$So_2 = \frac{K_1 + K_2 \bullet q}{K_3 + K_4 \bullet q} \quad (4)$$

where K_1, K_2, K_3 and K_4 are coefficients derived from the pulse oximeter calibration procedure that are related to the HbO_2 and RHb absorption coefficients.

2.2 Measurement system

The NIR laser diodes based pulse oximetry system[18,19] comprises an optical sensor, the sensor electronics, and the signal processing unit. The sensor consists of the optical emitters, photo-detectors and photo-detector pre-amplifier. Two laser diodes with peak wavelengths close to 750 nm and 850 nm, respectively, are used as optical emitters. To reduce the mismatch in both the pulsating and non-pulsating volumes probed by each wavelength and to minimize the movement artefacts, the two LD chips are mounted on a single metal heat sink with a separation distance between their central parts of 0.7 mm. Both chips are situated so that their emission beam larger divergence axes are parallel to the sensor central longitudinal axis. Taking this fact into account, three BPW34 p-i-n silicon photodiodes (PD) photo-detectors are connected in parallel. The first amplifier stage which converts the photocurrent into a proportional voltage is situated in the backside of the PD. The configuration of the optical sensor corresponds to the transmission mode. Thus, the emitters and the photo-detectors are situated in opposite sides, and should be placed in close contact with the peripheral vascular bed to be analyzed.

The laser diodes driver, amplification stages, timing and sample and hold circuits, constitute the sensor electronics. The laser diodes driver sequentially activates each LD with 5 μs pulses at a repetition rate of 1 kHz. The output voltage from the PD pre-amplified stage is further amplified and decomposed into separated channels using sample-and-hold circuits (S&H) synchronously triggered with respect to the pulse driving the corresponding LD. The outputs of the S&H are fed into the analogue inputs of a data acquisition board (12-bit DAQ1200, National Instruments). The timing board of the sensor electronics also generates the trigger and conversion signals for the acquisition board (DAQ). The DAQ and the processing programs installed on a handheld personal computer (Satellite 4000, Toshiba) constitute the signal processing unit. The S&H output signals are analogically pre-filtered by the DAQ with a simple anti-aliasing RC low pass filter at 300 Hz and are digitized at 1 kSa/s for every channel. The further stages of the signal processing are carried out through the previously reported algorithm[13-16].

2.3 Signal processing algorithm

The signal processing algorithm[13-16] relies on a numeric separation of E_{AC} and E_{DC} signals for both wavelengths and a non-linear filtering to calculate q (Eq. 3). The first operation performed on the raw measured data is a low pass filtering implemented with a ten-sample average algorithm. This pass reduces the amount of data by a tenfold and assures, in conjunction with the above mentioned hardware RC filtering, a correct anti-aliasing processing of the original signal. A flow of 100 Sa/s data is then fed to the following elaboration stages. Both channel streams of data, $E_1(t)$ and $E_2(t)$, are then digitally filtered to obtain the required E_{AC} and E_{DC} values. The E_{DC} is obtained by a low pass filtering, and E_{AC} by a pass-band one, followed by a peak-to-peak detector designed to reject signal spikes. The two linear filters, low pass and band pass, are obtained by a combination of two Bessel-type low pass filters.

Each input signal $E(t)$ signal is filtered by a low-pass filter of order n (being $n = 6$ in our case) and a low cut-off frequency LP, in order to obtain the constant value $E_{dc}(t)$ of the signal. After this stage, the signal $E_{dc}(t)$ is almost constant or non-variable over the period of the variable component of the PPG. In consequence, this value is directly suitable to be used as the E_{DC} parameter of expression (3). A similar filter, with order n and cut-off frequency HP is used to suppress high frequency components. The band-pass filtered signal $E_{ac}(t)$ is then obtained from the difference between the outputs of the two filters.

To obtain the peak-to-peak value of the pulsatile component E_{AC} a histogram reduction procedure[13, 15, 16] is applied. A frequency distribution of the data obtained after the band pass filtering ($E_{ac}(t)$) is computed for a define time interval. After that a fixed percentage of samples from both ends of such distribution or histogram are discarded. As the spikes appear in maxima and minima of the variable signal ($E_{ac}(t)$), the number of rejected points is similar in both extremes. The peak-to-peak value of the variable component E_{AC} is calculated from the difference between the maximum or higher value and the minimum or lower value of the reduced frequency distribution diagram. From the E_{DC} and E_{AC} components for each wavelength, we first calculate the q parameter, and then, the corresponding So_2 value using the expression obtained after the calibration procedure.

The algorithm has been implemented[16] using Lab Windows CVI™ facilities so that processing can be carried out both in real time and off-line (post-processing). In a user friendly manner, it is possible to set-up the Bessel filters cut-off frequencies, the histogram reduction parameters and the time processing interval. Additionally one can select the generation of files containing the 100 Sa/s PPG signals for both wavelengths, as well as the heart rate, *q* and saturation values obtained after all the processing. These options permit us to analyze the signals under different parameters, study the performance of the relation between *q* and So_2 and to adjust and optimize the processing conditions. The computer monitor displays all the fixed and derived parameters, as well as the obtained constant and variable components for both wavelengths.

3. TEST OF THE PROCESSING ALGORITHM

The photoplethysmography has been used for over more that 50 years and several studies have been devoted to the investigation of the PPG components[7-9, 22, 23]. It is assumed that the photoplethysmographic signal consists of two components, one pulsating in synchronism with the heart rate and a second one which fluctuates slowly, reflecting changes in total blood volume and in the tissue under study. The PPG cardiac synchronous component (0.67-3.33 Hz) is often referred to as the variable, while the second component usually is referred as the constant one. The variable signal is said to originate from smaller arteries and arterioles, but there are indications that the cardiac pulse is, indirectly or by arterio-venous shunts, transferred to the venous side of the circulation, which has a significant effect on the PPG signal as the veins are highly distensible and small pressure changes cause large blood volume fluctuations. In the called "constant" component of a PPG signal can be identified other fluctuations. The respiratory rate of adults at rest ranges from 5 to 24 min^{-1} (0.08-0.4 Hz) and that of neonates at rest ranges from 20 to 80 min^{-1} (0.17-1.33 Hz). In the frequency range below the respiratory rate can be found three sources of variations. The Traube-Hering-Mayer waves, which are caused by the sympathetic control of the tones of the vascular tree, have a fixed rate at about 0,1 Hz (0,09-0.11Hz). Variations associated with the body thermal regulation system (Burton waves) are seen in 0.03-0.05Hz. A 0.07-0.15 Hz component of more local origin is vasomotion and relaxation of small arteries, arterioles and venules (venomotion).

The signal pulsation of interest for deriving the oxygen saturation by pulse oximetry approach is generated by the beating heart. One can reasonably assume that its frequency will be over 0.5 Hz (i.e. 30 beats/min) and not exceed 5 Hz (i.e. 300 beats/min)[4]. Because of that, the filter frequency values are of the order of some tenths of Hertz for LP and in the range of 5 to 15 Hz for HP. We selected the Bessel filter over more sharp-edged filters as the Chebychev or Butterworth[24, 25] because of the higher linearity in phase response offered by the Bessel low pass filters, reflected in a smaller distortion in the shape of the PPG signals. The number or percentage of points rejected from the peak-to-peak $E_{ac}(t)$ histogram distribution is closely related to the signal spike type noise. This percentage should be obtained after a study of PPG signals. In order to test the influence of processing parameters like filters cut-off frequencies (LP, HP) and histogram reduction percentage (HR) on the derived *q* values, and indeed on the reported So_2 levels, PPG measured in pulsating beds of human volunteers have been analyzed and processed for different LP, HP and HR. To record the photoplethysmographic signals in stable conditions, the volunteers remained seated for some minutes and the transmittance sensor was attached to the distal part of a hand finger (in most cases the index finger). Once checked the sensor fixation and the quality of the signals, the raw 100 Sa/s PPG were recorded over at least 5 minutes for off-line processing.

For this study we selected three types of PPG signals in order to have a very stable PPG with an almost constant E_{DC} signal during the interval under study and PPG with different levels of E_{DC} signal changes. The measurement during apnoea operation is a good example for PPG with variable E_{DC} signal. The stable measurement was obtained from the transmittance PPG signals recorded in basal condition from a female volunteer hand finger[13] using a laser diode with peak emission at 850 nm, similar to the LD1 of the above described sensor. In figure 1 is shown a ten seconds raw PPG processed using different parameters in order to evaluate its influence on the signal. Figure 1a shows a 10 s PPG raw signal with the subtraction of the mean signal value for the exposed interval ($E-E_m$). Figure 1b represents the variable component obtained after Bessel filtering ($E_{ac}-E_{acm}$) having LP= 0.3 Hz and HP=10 Hz. Figure 1c exposes the effects of cutting away 10 % and 5 % of the points in the peak-to-peak histogram distribution (HR) of the 10 s interval signal values from the PPG of figure 1b. The results of applying HR=5% to the whole 10 s interval signal (Δt=10 s) compared with 2 s time intervals (Δt=2 s) are depicted in Fig. 1d. From figures 1a and 1b we can observe a better E_{DC} level stabilization after Bessel filtering which reduces the error for the peak-to-peak measurement. The use of a non linear filter with lower histogram reduction percentage (5%) reduces the spike influence for peak-to-peak measurement and no

cutting of the signal is observed (figure 1c). An increase of histogram reduction percentage to 10% produces the cut of the useful PPG signal for the highest and lowest values in the interval.

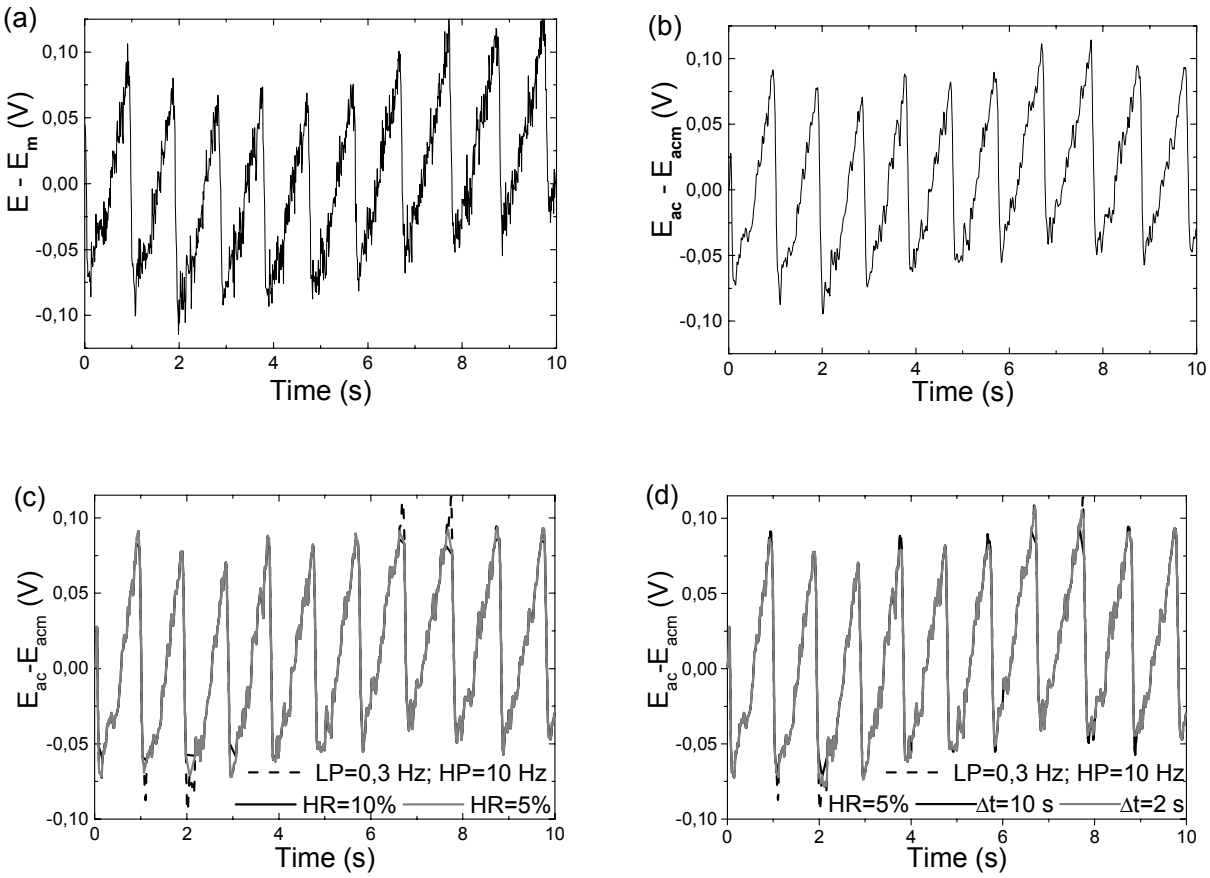

Figure 1. Transmittance PPG signal recorded in stable basal condition from the distal part of a female volunteer hand finger using a laser diode with peak emission at 850 nm. (a) Raw PPG signal after the subtraction of the mean signal value for the exposed interval ($E-E_m$). (b) PPG variable component obtained after filtering (cut-off frequencies LP= 0,3 Hz and HP=10 Hz). (c) The effects of cutting away 10 % and 5 % of the points in the peak-to-peak signal values histogram distribution (HR) over the whole 10 s interval. (d) The results of applying HR=5% to the whole 10 s interval signal (Δt=10 s) and over separated 2 s time intervals (Δt=2 s).

In order to choose the optimal Bessel filters cut-off frequencies we conducted a second study about the influence of these processing parameters on the obtained *q* values. A female healthy volunteer was monitored in stable basal conditions with the described transmittance sensor and system (see Section 2.2). The recorded transmittance PPG for both laser diodes LD1 and LD2 were analyzed through the application of Fast Fourier Transformation (FFT) and processed using the above-described algorithm (Section 2.3). In Fig. 2a and 2b are shown the LD1 and LD2 raw PPG recorded signals in two 30 s time intervals. In Fig. 2c and 2d are exposed the respective FFT performed on each time interval with the indication of the frequency values probably associated to cardiac activity, 1.17 Hz and 1.19 Hz, corresponding to 70.2 beat/min and 71.4 beats/min, respectively. In the second interval (370-400 s, Fig. 2b) is observed an oscillation of a frequency lower than the cardiac one in both PPG signals. The corresponding FFT (Fig. 2d) shows an increase of the amplitude values on both LD PPG at frequencies lower than 0.5 Hz. The *q* values were calculated from the LD1 and LD2 PPG signals for every two seconds according to Eq. 3 and the described processing algorithm, using different combinations of the cut-off frequencies (LP and HP) and peak-to-peak $E_{ac}(t)$ histogram reduction percentages (HR).

The q mean values (mean) and standard deviation (sd) were calculated for the time interval from 320 to 420, as well as for 320-350 s and 390-420 s. In Fig. 2e are shown the ratios of sd with respect to the mean (sd/mean)for the nine q combinations (*q10* to *q18*) of LP (0.1, 0.25, 0.5 Hz) and HP (5, 10, 15 Hz) as shown in the legend of Fig. 2e, being HR=5% (10 points rejected from 200, keeping 190 points) for the three time intervals. The smaller variation regardless of the time interval considered is observed in sd/mean for *q16*, which corresponds to LP = 0.5 Hz and HP = 10 Hz. The comparison of the results shown in the bar diagram (Fig. 2e) of LP = 0.5 Hz and HP = 10 Hz as the couple of parameters that gives similar q values in the three signal intervals.

To study PPG with large changes on E_{DC} signal a male healthy volunteer was monitored over several minutes with the transmittance sensor and system (Section 2.2), in stable basal conditions followed by an apnoea manoeuvre. The recorded transmittance PPG for both laser diodes LD1 and LD2 were analyzed through the application of FFT and processed using the described algorithm (Section 2.3). In Figure 3a are shown the LD1 and LD2 raw PPG signals recorded over a 220 s time interval (from 630 to 850 seconds), indicating with arrows the period of volunteer no breathing (apnoea). A large change of DC signal is observed as physiology response to the apnoea. This E_{DC} behaviour makes more difficult the signal processing in order to discriminate the E_{DC} and E_{AC} part In Fig. 3b and 3c are exposed the respective FFT performed on 30 s time intervals every 10 s on each LD PPG. These results show no large variations neither disparities from 5 to15 Hz in both LD, and changes over the time interval below 5 Hz. The q values for the combination of the LD1 and LD2 PPG signals were calculated for every two seconds according to Eq. 3 and the described processing algorithm, using different combinations of the cut-off frequencies (LP = 0.1, 0.25, 0.5 Hz and HP = 5, 10, 15 Hz) and peak-to-peak $E_{ac}(t)$ histogram reduction percentages (HR). The figures 4d, 4e and 4f reflect the behaviour patterns of the two seconds q values for different LP-HP combinations (*q10* to *q18*, as shown in the legend of Fig. 2e), being HR = 5 %, in the whole 630-850 s time interval, with the indication of the apnoea period. For comparison between graphics 4d-f, we can observe a small difference between PPG filtered with different high pass cut-off (5-15 Hz). However, for LP we observe a large difference, mainly for the increase of the q value. This increase is related with the decrease of oxygen saturation after a few minutes of apnoea. A higher value of q is obtained for a lower value of LP, changing from 1.6 for 0.1 Hz to 1.2 for 0.5 Hz. This large value disparity must be studied to select the optimal LP cut-off frequency, although the q values obtained with LP = 0.25 Hz (Fig. 3e) have a better coincidence with the apnoea manoeuvre.

4. DISCUSSION

The PPG measured for different persons under different conditions (basal, resting, during apnoea, exercise, etc.) present a large variety of shapes and signal frequencies. In order to optimise the signal processing to obtain the q value related to the oxygen saturation, for the most of measurement conditions and persons, we studied three cases of real photoplethysmographic signal that can represent a large variety of PPG. In a first case we have studied a PPG with a very stable E_{DC} and E_{AC} signals, typically of basal condition measurement. A second kind of PPG has intervals with a small low frequency fluctuation, that could be associated to small movement or fluctuation or to physiological changes. A third kind of PPG has large E_{DC} component changes, which represent measurements during movements and also with large changes on q value (as during apnoea manoeuvre).

The first case is shown in figure 1. The signal after band pass filtering (figure 1b) is filtered by the histogram reduction cutting away 10% or 5% of the interval points (figure 1c). By examination of the signal we observed a cutting excess in the signal interval extremes for HR = 10%. More appropriate cut is observed for HR = 5%, where only spike noise is removed. Similar results are observed for other PPG intervals. As the 10 s interval has signal fluctuations derived from the slow changes of E_{DC} component to the E_{AC} component, we reduced the signal interval to two seconds (figure 1d). For this lower time interval the HR = 5% is more effective and the influence of E_{DC} component is minimized. The combination of Δt = 2 s and HR = 5 % assures a good rejection of spikes without affecting the useful PPG signal.

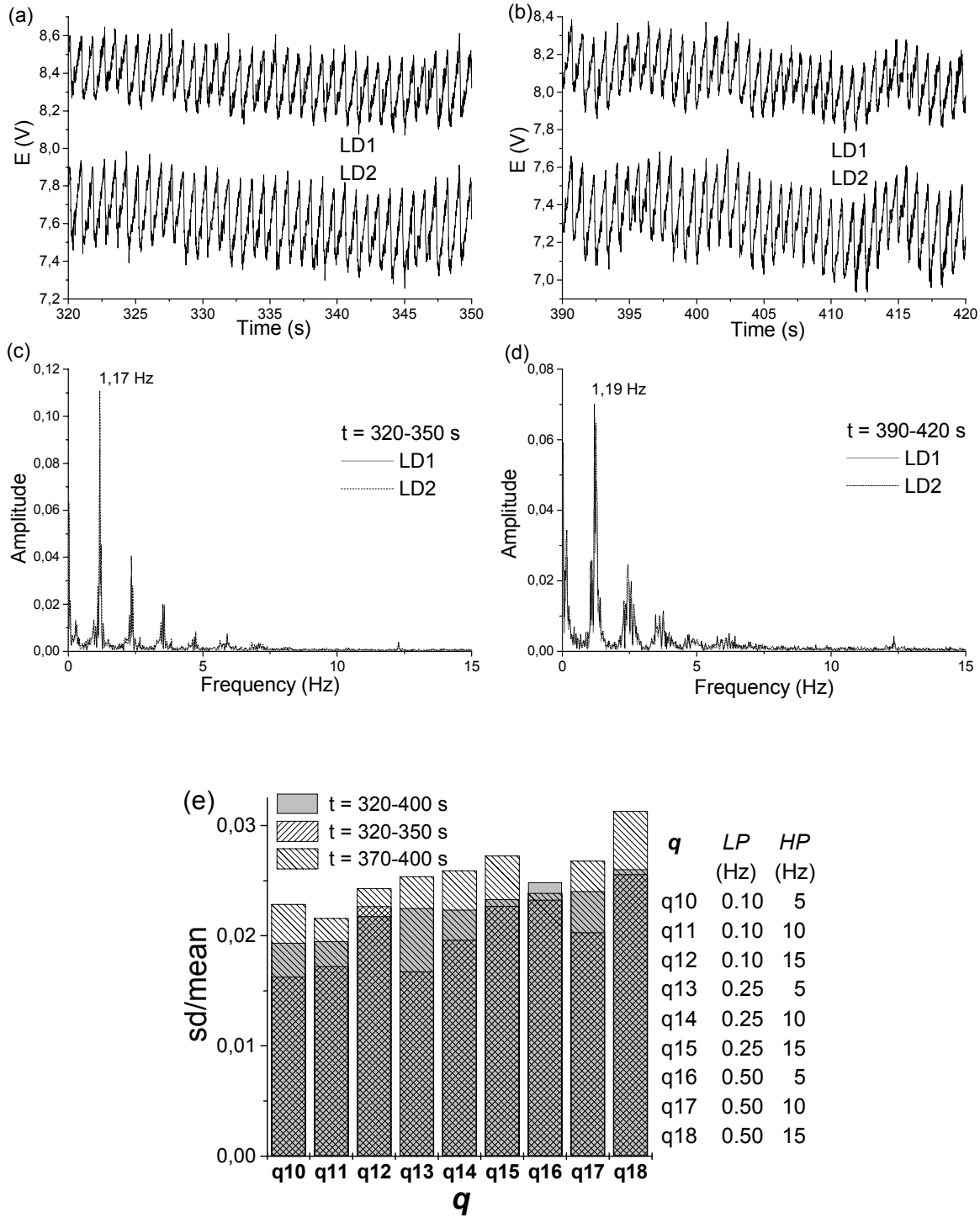

Figure 2. Transmittance PPG from two laser diodes LD1 and LD2. (a) LD1-PPG and LD2-PPG recorded in the time interval 320-350 s. (b) LD1-PPG and LD2-PPG recorded in the time interval 390-420 s. (c) LD1-PPG and LD2-PPG Fast Fourier Transformation for the time interval 320-350 s. (d) LD1-PPG and LD2-PPG Fast Fourier Transformation for the time interval 390-420 s. (e) Ratios of standard deviation (sd) and *q* mean values for different combinations of LP and HP, being HR = 5 %, in three time intervals.

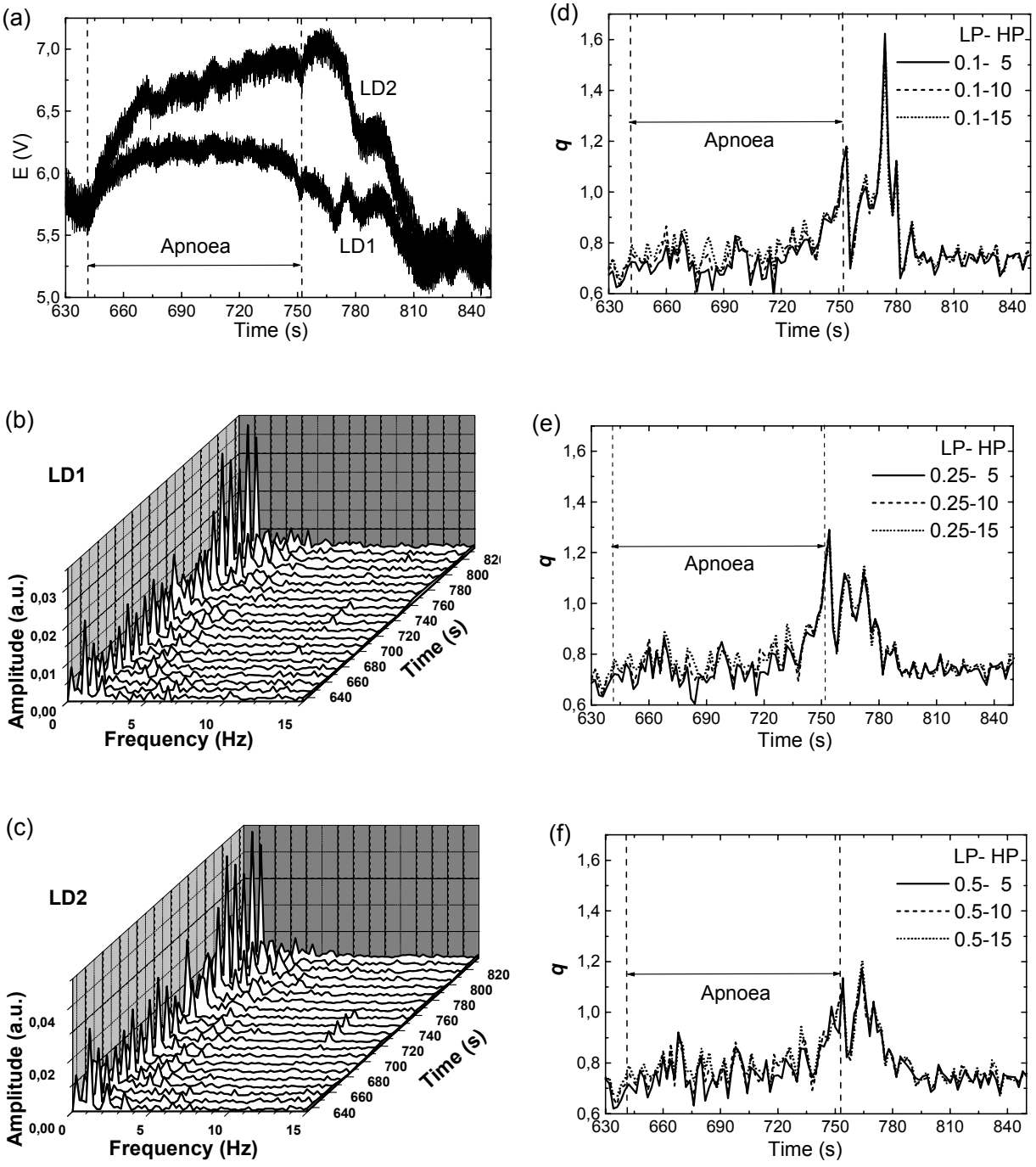

Figure 3. (a) LD1 and LD2 raw PPG signals recorded from 630 to 850 seconds indicating with arrows the period of volunteer no breathing (apnoea). (b) FFT performed on 30 s time intervals on LD1 PPG. (c) FFT performed on 30 s time intervals on LD2 PPG. (d) Two seconds *q* values obtained from LD1 and LD2 PPG signals processing for the combinations of cut-off frequencies LP = 0.1 Hz and HP = 5, 10, 15 Hz. (e) Two seconds *q* values obtained from LD1 and LD2 PPG signals processing for the combinations of the cut-off frequencies LP = 0.25 Hz and HP = 5, 10, 15 Hz. (f) Two seconds *q* values obtained from LD1 and LD2 PPG signals processing for the combinations of the cut-off frequencies LP = 0.5 Hz and HP = 5, 10, 15 Hz.

For PPG with E_{DC} fluctuation, as it is shown in figure 2b, we have studied the influence of filtering parameters on q values. We build a bar diagram with the values of standard deviation normalised to the mean q value for different LP and HP cut-off frequencies combination. This signal processing was applied to three PPG signal intervals with different E_{DC} fluctuations (t=320-400 s, t=320-350 s and t=370-400 s) shown in figures 2a and 2b. For comparison between the values obtained for each interval we observe for the couple 0.5 Hz and 5 Hz (LP and HP respectively) the most similar value of normalised standard deviation, that means the more uniform processing for all signal intervals.

From the two cases shown above, we have chosen the histogram reduction percentage, the length of the working interval and the cut-off frequency for the second low-pass Bessel filter (HP). After that we have studied the filtering in a PPG signal with large E_{DC} changes and also with changes in q value. In figures 3d-3f are shown the q values for different filtering parameters. For HP frequency only small changes are observed and no more information is obtained to choose the optimum value. For LP frequency we observe strong differences for each LP cut-off. For the lowest value of LP frequency, 0.1 Hz, the q value (1.6) is the highest. For this LP frequency the slow variation of E_{DC} component is added to the E_{AC} component increasing the q value. In the case of higher cut-off frequency (0.25 and 0.5 Hz) the q values are lower. The q values obtained with LP = 0.25 Hz (Fig. 3e) reflect the apnoea manoeuvre in a better way.

Some authors have analysed the characteristics of laser photoplethysmography in reflection mode [26-31]. When compared with a conventional photoplethysmograph, a signal derived from a laser contains a higher proportion of random signal superimposed on the pulse. The differences in results may depend on the differences in monochromatism and/or coherence of the light sources. The detailed optical and physical mechanism behind the generation of the PPG signal and its information content are complex and it is also present in a PPG derived from a laser source. When lasers are used as light sources, the signal becomes even more complicated. Laser light scattered from moving blood cells generates intensity changes in the photodetected signal. Erythrocyte orientation, blood volume variations, vessel wall motions and pressure-induced tissue motion may all contribute to the generation of the detected signal. Indeed new components unrelated in phase to the heart synchronous signal are added and will affect the amplitude of the heart synchronous signal in a way which is unpredictable.

In the reflection mode, the signal is determined mainly by the superficial vasculature, whereas in the transmission mode, the whole volume between the light source and the photodetector has to be considered. Transmission mode may be an alternative, even if the number of measuring sites are more limited. This mode may have some advantages, e.g., the monitored vascular volume increases and many more different types of vessel will be represented in the volume under study. Thus the signal intensity increases, which may result in a better signal/noise ratio. However, in the case of transmittance with laser diodes to probe more different types of vessel in the volume under study could represent more sources of variations in the detected signal. The signals detected in a finger by a transmittance laser diodes sensor will monitored the contributions from different vascular beds such as high density small arteries and arterioles, as well as from the large number of complex arteriovenous anastomoses, located some of them at a deep vascular level. Further to it, the light must travel a greater distance through the tissue which increases the probability of multiple scattering from other tissue structures.

Another possible source of noise is laser radiation reflected or backscattered from the analysed vascular bed. The reflected or backscattered radiation can produce an optical feedback in the laser that may be detrimental to laser diode operation. For certain feedback levels, instabilities occur with noise and increase of spectral line-width. For optical feedback level as lower as 10^{-6} these instabilities appears by the presence in the laser cavity of radiation with different phase. In our case the optical feedback comes back after different scattering process in different parts of the tissue promoting an increase of the noise. This can be the origin of the large number of spikes that we measured with our system. Changes on the optical system can reduce this perturbation.

As result of our studies we can conclude that the processing of the transmittance laser diode PPG signal can be improved by averaging several pulses, followed by the application of Bessel filtering and a non-linear filtering. The selection of the linear filters cut-off frequencies and non-linear filter parameters in conjunction with the analysis in small working interval, let to reject the signal spikes and to derive more efficiently the variable and constant components of the PPG signals. After that it possible to perform a more accurate determination of the q value related to the oxygen saturation value.

5. ACKNOWLEDGEMENTS

The authors would like to express their gratitude to Dr. Romano Gianneti for providing the processing programs and the assistance in the data processing. This work has been partially supported by the Spanish CICYT project TIC98-1025. SMLS is supported by *Programa Ramón y Cajal* from the Spanish Ministry of Science and Technology.

6. REFERENCES

1. T. Aoyagi, M. Kishi, K. Yamaguchi and S. Watanabe, "Improvement of an earpiece oximeter", In: *Abstracts of the Japanese Society of Medical Electronics and Biological Engineering*, pp. 90-91 (1974).
2. I. Yoshiya, Y. Shimada and K. Tanaka, "Spectrophotometric monitoring of arterial oxygen saturation in the fingertip", *Med. Biol. Eng. Comp.* **18**, 27-32 (1980).
3. I. Yoshiya and Y. Shimada, "Non-invasive spectrophotometric estimation of arterial oxygen saturation". In: *Noninvasive physiological measurements*, Academic, New York, pp. 251-286 (1983).
4. J. A. Pologe, "Pulse oximetry: Technical aspects of machine design*", Int. Anesthesiol. Clin.* **25**, 137-153 (1987).
5. Y. Mendelson, "Pulse oximetry: theory and applications for noninvasive monitoring*", Clin. Chem.* **38**, 1601-1607 (1992).
6. L. G. Lindberg, C. Lennmarken and M. Vegfors, "Pulse oximetry - clinical implications and recent technical developments", *Acta Anesthesiol. Scand.* **39**, 279-287 (1995).
7. Nijboer, J.C. Dorlas and H.F. Mahieu, "Photoelectric plethysmography. Some fundamental aspects of the reflection and transmission method", *Clin. Phys. Physiol. Meas.* 2, pp. 205-215, 1981.
8. J. Giltvedt, A. Sira and P. Helme, "Pulsed multifrequency photoplethysmograph", *Med. Biol. Eng. Comp.* 22, pp. 212-215, 1984.
9. A.A.R. Kamal, J.B. Harness, G. Irving and A.J. Mearns, "Skin photoplethysmography - a review", *Comp. Methods Programs Biomed.* 28, pp. 257-269, 1989.
10. E. J. Van Kampen and W. G. Zijlstra, "Spectrophotometry of hemoglobin and hemoglobin derivatives", *Adv. Clin. Chem.* **23**, 199-257 (1983).
11. A. Zwart, E. J. Van Kampen and W. G. Zijlstra, "Results of routine determination of clinically significant hemoglobin derivatives by multicomponent analysis", *Clin. Chem.* **32**, 972-978 (1986).
12. W. G. Zijlstra, A. Buursma and W. P. Meeuwsen van der Roest, "Absorption spectra of human fetal and adult oxyhemoglobin, deoxyhemoglobin, carboxyhemoglobin and methemoglobin", *Clin. Chem.* **37**, 1633-1638 (1991).
13. S. M. López Silva, "Oximetría de pulso con diodos láser infrarrojos", *Tesis Doctoral*, Universidad Complutense de Madrid (1997).
14. S. M. López Silva, R. Giannetti, M. L. Dotor, J. R. Sendra, J. P. Silveira and F. Briones, "Application of NIR laser diodes to pulse oximetry", In *Biomedical Sensors, Fibers, and Optical Delivery Systems*, Francesco Baldini, Nathan I. Croitoru, Ingemar Lundström, Mitsunobu Miyagi, Ricardo Pratesi, Otto S. Wolfbeis, Editors, *Proc. SPIE* **3570**, 294-302 (1998).
15. R. Giannetti, S. M. López Silva, M. L. Dotor, J. R. Sendra, J. P. Silveira and F. Briones, "An innovative signal processing algorithm for near infrared laser-based pulse oximeter", *Proc. IMEKO TC-4*, 153-156 (1998).
16. R. Giannetti, S. M. López Silva, M. L. Dotor, J. R. Sendra, J. P. Silveira, D. Golmayo and F. Briones, "Real time processing algorithm for a new NIR laser pulse oximeter", *Proc. ESEM-99*, 217-218 (1999).
17. J. P. Silveira, S. M. López Silva, M. L. Dotor, D. Golmayo, R. Giannetti, J. R. Sendra y J. L. Alvarez-Salas, "Oximetría de pulso basada en diodos láser infrarrojos", *Libro de Actas de CASEIB 2000*, 13-16 (2000).
18. S. M. López Silva, J. P. Silveira, J. R. Sendra, R. Giannetti, M. L. Dotor and D. Golmayo, "NIR transmittance pulse oximetry system with laser diodes", In *Clinical Diagnostic Systems*, Gerald E. Cohn, Editor, *Proc. SPIE* **4255**, 80-87 (2001).
19. S. M. López Silva, J. P. Silveira and M. L. Dotor (submitted to JBO).
20. W. G. Zijlstra and B. Oeseburg, "Definition and notation of hemoglobin saturation", *IEEE Trans. Biomed. Eng.* **36**, 872 (1989).
21. Y. Mendelson and J. C. Kent, "Variations in optical absorption spectra of adult and fetal hemoglobin and its effects on pulse oximetry", *IEEE Trans. Biomed. Eng.* **36**, 844-848 (1989).

22. L.G. Lindberg, H. Ugnell and P.A. Öberg, "Monitoring of respiratory and heart rates using a fibre-optic sensor", *Med. Biol. Eng. Comp.* 30, pp. 533-537, 1992.
23. A. Johansson, *Photoplethysmography in multiparameter monitoring of cardiorespiratory function*, Dissertation 629, Department of Biomedical Engineering, Linköping University, Sweden, 2000.
24. Y. Mendelson and B. Ochs, "Noninvasive pulse oximetry utilizing skin reflectance photoplethysmography", *IEEE Trans. Biomed. Eng.* 35, pp. 798-805, 1988.
25. J.P. De Kock, *Pulse oximetry: theoretical and experimental models*, D. Ph. Dissertation, University of Oxford, UK, 1991.
26. N.E. Almond and E.D. Cooke, "Observations on the photoplethysmograph pulse derived from a laser Doppler flowmeter", *Clin. Phys. Physiol. Meas.* 10, pp. 137-145, 1989.
27. N.E. Almond and E.D. Cooke, "Comments on photoplethysmograph noise", *Clin. Phys. Physiol. Meas.* 10, pp. 367-368, 1989.
28. N.E. Almond and E.D. Cooke, "Photoplethysmograph from a laser source", *Med. Biol. Eng. Comp.* 29, pp. 564, 1991.
29. L.G. Lindberg, T. Tamura and P.A. Öberg, "Photoplethysmography. Part 1. Comparison with laser Doppler flowmetry", *Med. Biol. Eng. Comp.* 29, pp. 40-47, 1991.
30. L.G. Lindberg and P.A. Öberg, "Photoplethysmography. Part 2. Influence of light source wavelength", *Med. Biol. Eng. Comp.* 29, pp. 48-54, 1991.
31. L.G. Lindberg and P.A. Öberg, "Photoplethysmograph from a laser source", *Med. Biol. Eng. Comp.* 29, pp. 568, 1991.